Available online at www.sciencedirect.com

ScienceDirect

Ceramics International 40 (2014) 1873–1878

CERAMICS INTERNATIONAL

www.elsevier.com/locate/ceramint

Grain boundary character distributions of sigma2 boundaries in WC–Co composites with different cobalt volume fractions

Xiaokun Yuan*

College of Materials Science and Engineering, Beijing University of Technology, Beijing 100124, China

Received 25 April 2013; received in revised form 5 July 2013; accepted 20 July 2013
Available online 26 July 2013

Abstract

The grain boundary character distributions of sigma2 grain boundaries were investigated in WC–Co samples with different cobalt volume fractions. Specimens were prepared with cobalt fractions of 6 wt%, 8 wt% and 10 wt% respectively. The electron backscattered diffraction measurements show that with the increase of the cobalt fraction, the population of sigma2 boundaries decreases and sigma2 twist boundary keeps as the most common boundary type. The result suggests that the cobalt volume fraction could be determinant in controlling the population of sigma2 grain boundaries in cemented carbides.

Keywords: A. Sintering; B. Electron microscopy; B. Grain boundaries; D. Carbides

1. Introduction

It is known that if the types of grain boundaries in polycrystalline materials can be controlled, certain properties can be improved, and this practice has come to be known as "grain boundary engineering" (GBE) [1]. Many reports on grain boundary engineered materials cite the enhanced proportion of low-sigma coincidence site lattice (CSL) boundaries, where sigma value is the reciprocal density of coinciding sites, as the factor responsible for property improvements. In addition to sigma3^n CSL boundaries in cubic metals and alloys, sigma2 boundary in hexagonal materials, i.e. tungsten carbide [2], is attracting special interest. The sigma2 boundary can be described as a 90 degree rotation about the [10–10] axis abbreviated as 90°/[10–10], which is thought to have low interfacial energy and high work of separation [3]. Note that the c/a ratio of WC is 0.976, therefore, sigma2 boundary is actually an "approximate" or "near" CSL boundary.

Further understanding of the GBE mechanisms requires an in-depth knowledge of grain boundary structure. The electron backscattered diffraction (EBSD) technique is an effective way to study the CSL boundaries on a more statistical volume basis. In recent years, there are increasing studies that focus on the sigma2 boundaries by virtue of EBSD technique [4–8]. The EBSD technique describes the lattice misorientation across the boundary via three Eulerian angles. To provide a more comprehensive description of the grain boundary character distribution (GBCD) within a polycrystal, specification about the grain boundary orientation by two spherical angles is needed [4,7].

Typical WC–Co composites (namely cemented carbides) used in industries normally contain 6–15 wt% cobalt as binder phase. Nevertheless, there are limited literatures concerning how the population of sigma2 boundaries alters with the variation of cobalt fractions. Therefore, the objective of current work is to study how the sigma2 boundary population is sensitive to cobalt volume fraction, under the condition that processing parameters other than cobalt volume fraction are kept nominally the same.

2. Experimental

Three specimens are used in this work and are prepared by two steps. First, the WC–Co composite powder was synthesized by in-situ reduction and carbonization reactions from tungsten oxide powder containing cobalt oxide. Second, the WC–Co composite powder was sintered into WC–Co bulks by sintering in hot

*Tel./fax: +86 10 67396260.
E-mail address: yuanxiaokun@bjut.edu.cn

0272-8842/$ - see front matter © 2013 Elsevier Ltd and Techna Group S.r.l. All rights reserved.
http://dx.doi.org/10.1016/j.ceramint.2013.07.091

isostatic pressing (Sinter-HIP) at 1500 °C for 30 min in a 6 Mpa argon atmosphere. Sample 1 (similarly hereinafter) has a cobalt fraction of 6 wt%, while sample 2 (similarly hereinafter) and sample 3 (similarly hereinafter) have cobalt fraction of 8 wt% and 10 wt% respectively. The specimens are with no intentional alloying additions, and with an average grain size of about 1 μm. The fracture toughness of the samples was measured on a MTS 810 material test machine.

The samples were then treated for EBSD analysis by polishing with a diamond abrasive and etching in Murakami's reagent for not more than 5 s. This treatment preferentially attacked cobalt phases and thus yielded WC surfaces suitable for EBSD mapping. The EBSD measurements were performed by a high speed EDAX Hikiari camera incorporated in a FEI Quanta 250 scanning electron microscope. To ensure the accuracy of the measurements, the EBSD data were collected with a step size of 0.1 μm.

As the first step in data processing, the original EBSD data underwent a cleanup procedure to correct spurious pixels that result from the incorrect indexing. Then for each specimen, the microstructures was indicated by the image quality (IQ) map, the orientation relationship between carbide grains was revealed by the misorientation angle distribution, the orientation texture of carbide/carbide boundaries was characterized by the misorientation distribution function (MDF), and the orientation texture of sigma2 boundary planes was represented by the grain boundary plane orientation distribution function (GBP-ODF). The data processing was performed by EDAX OIM Analysis 5.3 software; the GBP-ODF module in the OIM software was developed under the auspices of the MRSEC at Carnegie Mellon University; the Brandon criterion [9] was used to determine the fraction of sigma2 boundaries.

3. Results and discussion

The image quality (IQ) maps are used to illustrate the microstructures of the samples, as shown in Fig. 1, with sigma2 boundaries highlighted in red. As indicated by the Figure, the three specimens exhibit microstructures with continuous skeleton of prismatic WC grains embedded in the cobalt binder phases. Note that for each specimen, only a selected measurement region is illustrated in Fig. 1. Moreover, the Σ2 boundary traces are calibrated on the noise-reduced and cleaned data. However, several traces that conform the misorientation relationship of Σ2 boundary can still be observed inside certain grains. One plausible explanation about this phenomenon is that there are limited slip systems in close packed hexagonal lattice, and thus high strain rate during sample preparation might cause pseudo-symmetry and deformation twins. Nevertheless, the mis-indexed boundary traces in each specimen are not prevalent and only occupy less than 3% of the overall length of carbide/carbide boundaries. Therefore, it is assumed that the mis-indexed boundary traces have limited effect on the statistics of the Σ2 boundary population. Also note that during sample preparation, most of the cobalt phases were attacked and removed by Murakami's reagent. In this case, to illustrate the increase of cobalt fraction in the samples, the length of carbide/cobalt boundary segments per square micron in the three specimens were counted, and the results are 1.145 μm for sample 1, 1.429 μm for sample 2, and 1.562 μm for sample 3. Using the length fraction of carbide/cobalt boundary segments as the proxy of the volume fraction of cobalt phases, the increase of cobalt fraction in the samples can therefore be identified.

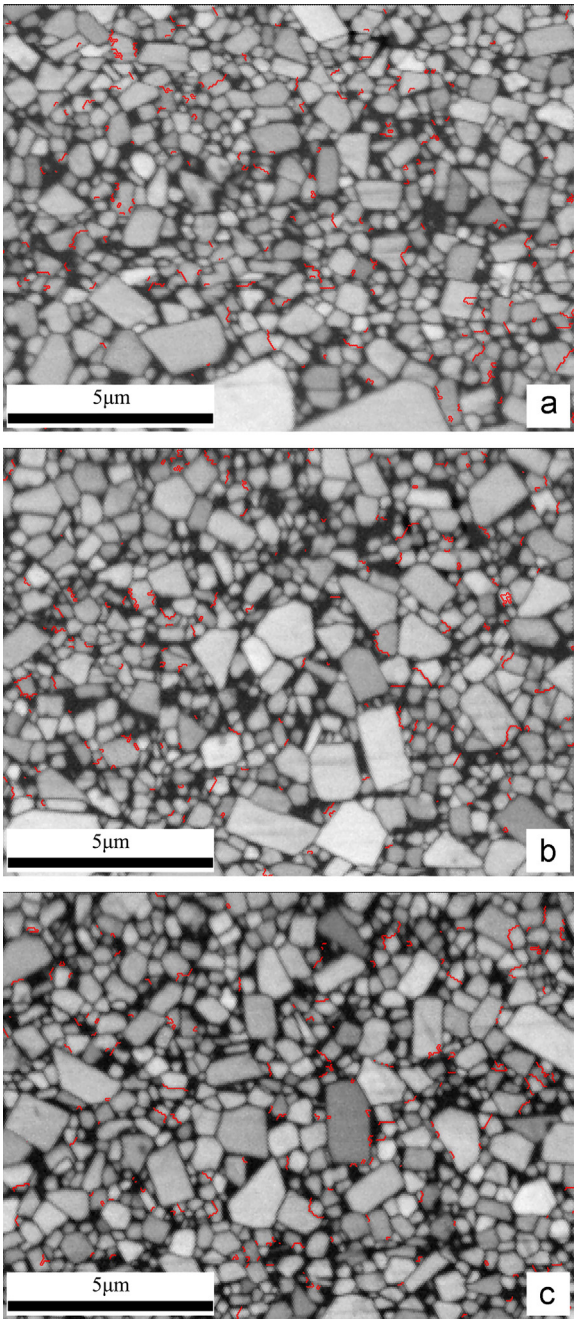

Fig. 1. Image quality maps of the partial measurement regions, with sigma2 boundaries highlighted in red, (a) sample 1; (b) sample 2; and (c) sample 3. (For interpretation of the references to color in this figure legend, the reader is referred to the web version of this article.)

To analyze the orientation relationship between carbide grains, the misorientation angle distributions were calculated and illustrated in Fig. 2. In this chart, the black line represents the misorientation distribution for an ideally random microstructure

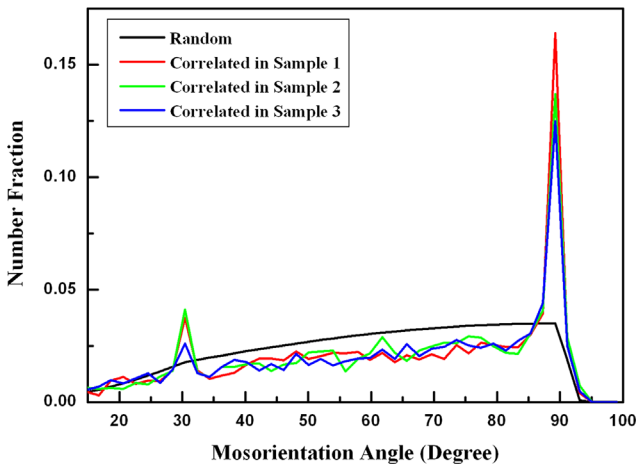

Fig. 2. Grain boundary populations of WC crystals and a random objects as a function of misorientation angle.

[10], while the colored lines show the misorientation distributions for the grain boundaries in each specimen. It can be seen that the experimental distributions are clearly not random, and there is an obvious misorientation angle preference corresponding to the sharp peaks at 90°. Moreover, with the increase of cobalt fraction, such preference decreases clearly.

To examine the orientation texture of carbide/carbide boundaries, the data are plotted in axis–angle space, and the outcomes of the three samples, namely the axis/angle MDFs, are shown in Fig. 3, with units of the contours in multiples of random distribution (MRD). A larger MRD value indicates a relatively stronger preference of the rotation axis. Note that for a complete axis/angle space, the misorientation angle describes the rotation angle of the grain boundary, and the azimuthal and polar angles describe the rotation axis of the grain boundary. As illustrated in Fig. 3, for the three samples, the strongest peak is at [10–10] axis for rotations of 90°, indicating that [10–10] is the dominant misorientation axis, and boundaries with such misorientation occur most frequently. However, although the axis/angle MDF configurations of the samples are quite similar, the maximal at the 90°/[10–10] positions differ, with 15.384 MRD for sample 1, 14.473 MRD for sample 2 and 13.846 MRD for sample 3. By comparing these maximum MRD values, it can be estimated that there is about 10% reduction in the number of sigma2 boundaries when the cobalt fraction develops from 6 to 10 wt%.

In OIM software, there is a kind of length-based definition of aspect ratio, which is given by the ratio of the minor axis length to the major axis length of an ellipse that fitted to the contour of a certain grain according to the least square method, thus, the aspect ratio value ranges from 0 to 1. This aspect ratio is named as "grain shape aspect ratio", and its descriptive geometry is illustrated in Fig. 4. The carbide grain populations as a function of grain shape aspect ratio in the three samples were calculated and the outcomes are presented in Fig. 5. In the chart, there is a predominant aspect ratio with an approximate value of 0.62 for each specimen, meantime, as carbide volume fraction increases, carbide grains with such aspect ratio occupy higher number fractions (19% for sample 1, 26% for sample 2, and 53% for sample 3). One issue needs attention, that is, very differently shaped grains (for example,

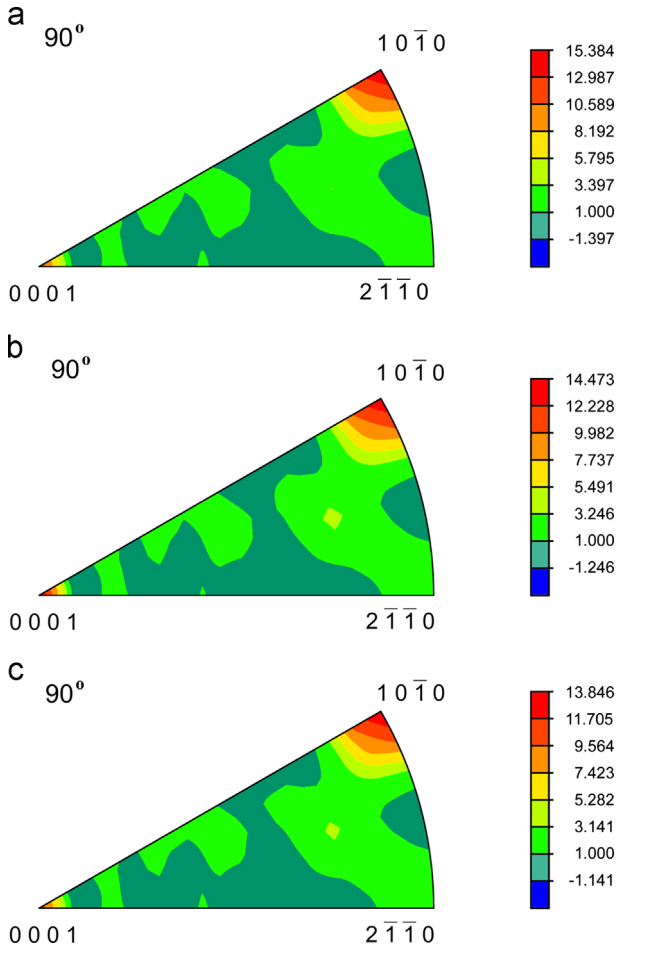

Fig. 3. The misorientation distribution functions in axis–angle space, for illustrating the orientation texture of carbide/carbide boundaries, with units of the contours in MRD, (a) sample 1; (b) sample 2; and (c) sample 3.

grains with square or elongated configuration) can have the same aspect ratio value, in the square cases, the methodology in OIM software preserves the aspect ratio that fits along the diagonal. Therefore, although the population of "0.62 ellipse" might be used as an index of carbide grain shape anisotropy, the results in Fig. 5 can merely roughly indicate the effect of cobalt fraction on the shape anisotropy of carbide grains.

There are two kinds of interfaces in cemented carbides: one is the phase boundary between carbide and cobalt phases, and the other is the grain boundary between carbide grains. In this work, we merely concentrate on the carbide/carbide boundaries. Previous work [11] reports that the most common carbide/carbide boundary planes have (0001) and (10–10) orientations. The GBP-ODF of sigma2 boundary planes is conducted by examining the grain boundary plane orientation at the specific misorientations of 90°/[10–10], and the outcome is illustrated in a stereographic projection, as shown in Fig. 6, with units of the contours in MRD. For each sample, the distribution peak of sigma2 boundary plane orientation in Fig. 6 is at the position of the misorientation axis [10–10], indexed as an oval, which means that the sigma2 boundary plane is perpendicular to the common rotation axis. Therefore, sigma2 boundary has a twist configuration that consists of (10–10) prismatic planes in both grains. Meantime, the absence

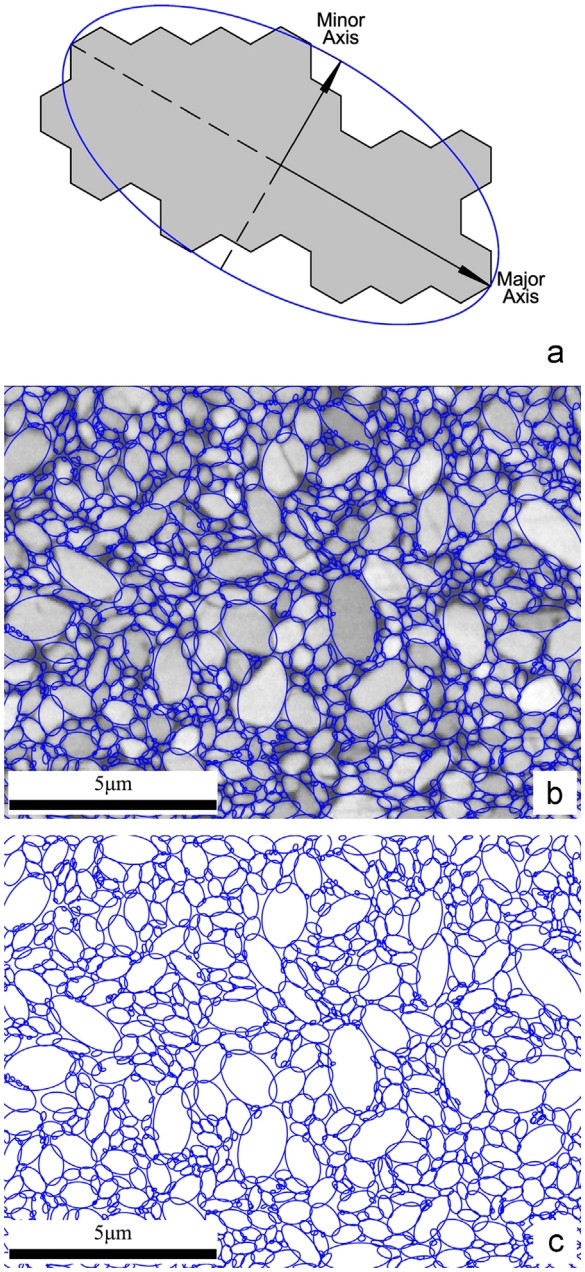

Fig. 4. The carbide grain shape ellipses highlighted in blue that fit to the contour of carbide grains, (a) the descriptive geometry; (b)shape ellipses imposed on carbide grains (taken sample 3 as an example); and (c) shape ellipses distribution. (For interpretation of the references to color in this figure legend, the reader is referred to the web version of this article.)

of a peak along the great circle perpendicular to the [10–10] misorientation axes (where the hexagon lies) indicates that sigma2 boundary seldom has a tilt configuration that consists of a (0001) basal plane in one grain against a (10–10) prismatic plane in the other. Note that a larger MRD value indicates a relatively higher occurring frequency (taken the relative area as the proxy) of the corresponding boundary type. Accordingly, the relative areas of sigma2 twist boundaries are 280 MRD in sample 1, 220 MRD in sample 2, and 195 MRD in sample 3, which also suggests that the relative area of sigma2 boundaries decreases with the increase of the cobalt fraction.

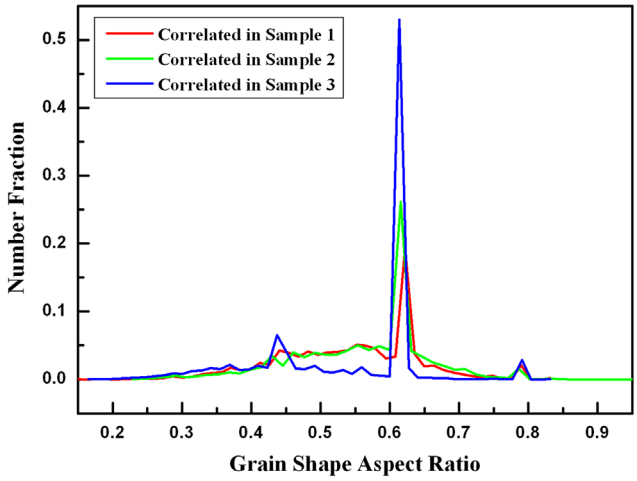

Fig. 5. Carbide grain populations as a function of grain shape aspect ratio.

The findings of present study demonstrate that in a range of different carbide volume fraction, the occurring frequencies of sigma2 boundaries differ, indicating that the carbide volume fraction may serve to control the population of sigma2 boundaries. Considering the preparation method of the specimens in this work, the sigma2 boundaries could either be in existence at WC–Co composite powder stage, or be evolved during the sintering procedure for bulk samples. Previous study [5] states that there might be a decrease of sigma2 boundary concentration from initial condition towards equilibrium state. Another reference [12] also regards that the decrease of sigma2 boundary fraction happens along with the rapid grain growth at early stages of sintering. Considering the situation in this work, the cemented carbide bulks were sintered from the same in-situ synthesized WC–Co composite powder. So how the cobalt volume fraction impact the population of sigma2 boundaries during the sinter-HIP process is mainly concerned.

The cobalt phase in cemented carbides can exist in two allotropic forms, that is, hcp or fcc [13], and the hcp form of cobalt can be stabilized and retained to a large degree in the cemented carbide. The 1500 °C sintering temperature of sinter-HIP in current work is higher than the melting point of cobalt phase (1495 °C). Higher cobalt fraction means Co need not to travel long distance to wet and cover WC particles, meantime, it is easy for cobalt to link between WC phases by virtue of capillary force and to form the thin layer structure on WC surface. Furthermore, if there is more cobalt phase in the vicinity of the WC grains in the sintered bulk, the stress at the general carbide/carbide boundaries can be more easily released through the local deformation of cobalt phase, which can result in higher fracture toughness. This is consistent with the experiment results (the fracture toughness is 13.95 MPa $m^{1/2}$ for sample 1, 16.08 MPa $m^{1/2}$ for sample 2, and 16.50 MPa $m^{1/2}$ for sample 3).

Fig. 6 overall suggests that the population of sigma2 boundaries generally decreases with increased cobalt fraction, and particularly, the sigma2 twist boundary is the most common boundary type in the studied samples. An earlier study [14] reports that the sigma2 twist boundary has an interface energy one order of magnitude

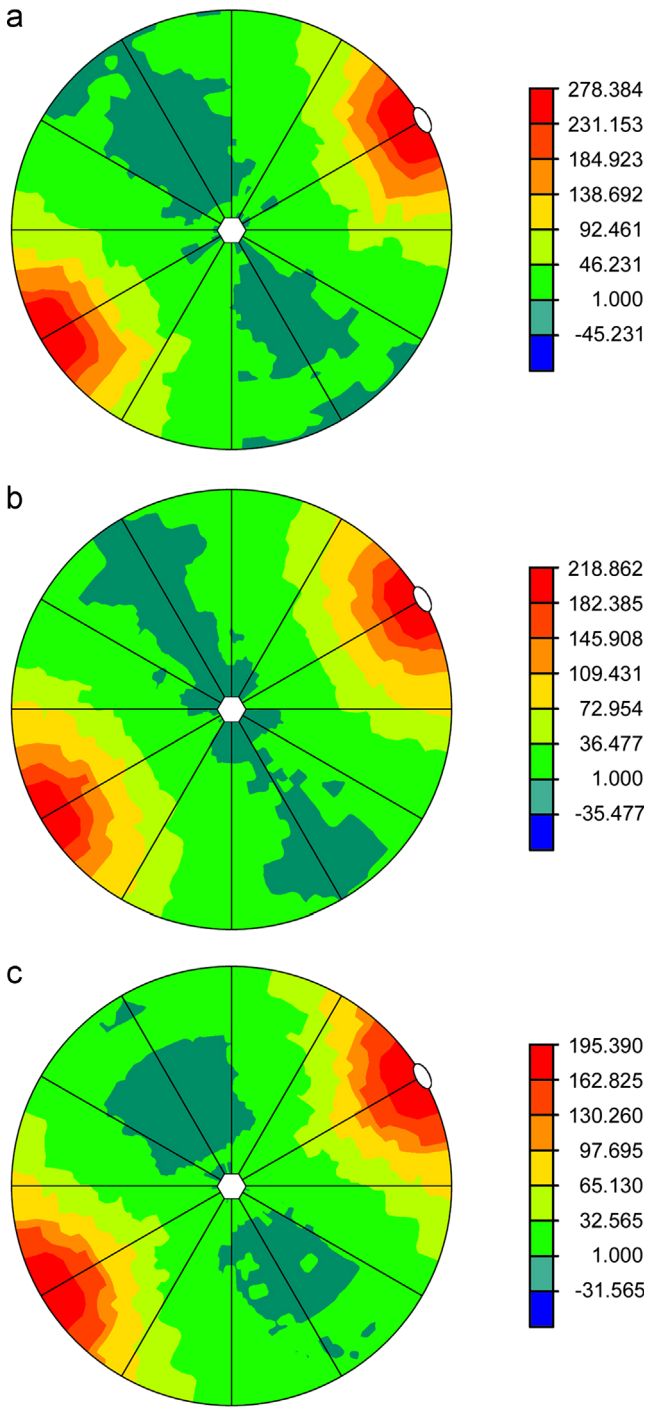

Fig. 6. Orientation distribution functions of sigma2 grain boundary planes, with units of the contours in MRD, (a) sample 1; (b) sample 2; and (c) sample 3.

lower than that of the sigma2 tilt boundary, and hence, the sigma2 twist boundary is a kind of strong interface, in other words, it is stable and is quite difficult for cobalt phase to reside in, and particularly, it is usually not wetted by the cobalt phases during sintering, which has been proved by both microanalysis experiment [15] and theoretical calculation [3]. Therefore, current observation suggests that higher cobalt volume fraction might accelerate the elimination of sigma2 boundaries. Possible routines of sigma2 elimination may include coalescence of the subgrains, shear transformation, grain rotation, as well as diffusional mechanisms [5]; however, detailed studies are needed to illustrate the role of cobalt volume fraction on these possible mechanisms.

An earlier study [7] finds that the sigma2 boundary populations do not vary with carbide volume fraction; moreover, the population of sigma2 boundaries is determined by the grain boundary energy anisotropy. Although the outcomes of reference [7] and current study differ, it is difficult to say whether this difference in occurrence is significant, since not only different starting materials and sintering temperatures were focused, but also the concentration of sigma2 boundaries are studied from a combined data set in reference [7]. As mentioned earlier, cobalt volume fraction could influence the contact situation of carbide phase in the starting material, so, it could in turn influence the boundary evolution towards the steady state that is determined by the relative boundary energies, and this may be the part of explanation for the difference.

4. Conclusions

The geometric and crystallographic characteristics of sigma2 grain boundaries in WC–Co composites with a range of carbide volume fractions have been characterized. Sigma2 twist boundary remains as the most frequently occurring boundary type, meanwhile, its population decreases with the increase of cobalt fraction. The result suggests that the cobalt volume fraction could be determinant to control the population of sigma2 grain boundaries in cemented carbides.

Acknowledgments

Prof. Gregory S. Rohrer from Carnegie Mellon University MRSEC, is especially appreciated for helpful discussions. The author's colleague, Dr. Yuntao Lei, is also thanked for providing kind help to this work. Supports from Chinese National Programs for Fundamental Research and Development 2011CB612207 and Beijing Natural Science Foundation 2123061, were also acknowledged.

References

[1] T. Watanabe, Grain boundary engineering: historical perspective and future prospects, Journal of Materials Science 46 (12) (2011) 4095–4115.
[2] S. Hagege, G. Nouet, P. Delavignette, Grain boundary analysis in TEM (IV) coincidence and the associated defect structure in tungsten carbide, Physica Status Solidi A 62 (1) (1980) 97–107.
[3] M. Christensen, G. Wahnstrom, Co-phase penetration of WC(10–10)/WC (10–10) grain boundaries from first principles, Physical Review B 67 (11) (2003) 115415/1–11.
[4] C.S. Kim, G.S. Rohrer, Geometric and crystallographic characterization of WC surfaces and grain boundaries in WC–Co composites, Interface Science 12 (1) (2004) 19–27.
[5] V. Kumar, Z.Z. Fang, S.I. Wright, An analysis of grain boundaries and grain growth in cemented tungsten carbide using orientation imaging microscopy, Metallurgical and Materials Transactions A 37 (3) (2006) 599–607.

[6] G. Ostberg, M.U. Farooq, M. Christensen, H.O. Andren, U. Klement, G. Wahnstrom, Effect of Σ2 grain boundaries on plastic deformation of WC–Co cemented carbides, Materials Science and Engineering: A 416 (1-2) (2006) 119–125.
[7] C.S. Kim, T.R. Massa, G.S. Rohrer, Interface character distributions in WC–Co composites [J], Journal of the American Ceramic Society 91 (3) (2008) 996–1001.
[8] K. Mannesson, M. Elfwing, A. Kusoffsky, S. Norgren, J. Agren, Analysis of WC grain growth during sintering using electron backscatter diffraction and image analysis, International Journal of Refractory Metals and Hard Materials 26 (5) (2008) 449–455.
[9] D.G. Brandon, The structure of high-angle grain boundaries, Acta Metallurgica 14 (11) (1966) 1479–1484.
[10] J.K. Mackenzie, M.J. Thomson, Some statistics associated with the random disorientation of cubes, Biometrika 44 (1–2) (1957) 205–210.
[11] Y. Zhong, H. Zhu, L.L. Shaw, R. Ramprasad, The equilibrium morphology of WC particles—a combined ab initio and experimental study, Acta Materialia 59 (9) (2011) 3748–3757.
[12] J.D. Kim, S.J. Kang, J.W. Lee, Formation of grain boundaries in liquid phase sintered WC–Co alloys, Journal of the American Ceramic Society 88 (2) (2005) 500–503.
[13] K.P. Mingard, B. Roebuck, J. Marshall, G. Sweetman, Some aspects of the structure of cobalt and nickel binder phases in hardmetals, Acta Materialia 59 (6) (2011) 2277–2290.
[14] M. Christensen, G. Wahnstrom, Effects of cobalt intergranular segregation on interface energetics in WC–Co, Acta Materialia 52 (8) (2004) 2199–2207.
[15] J. Vicens, E.L. Pinson, J. Chermant, G. Nouet, Structural analysis and properties of grain boundaries in hexagonal carbides, Journal de Physique 49 (5) (1988) 271–276.